J. Fluid Mech. (1981), *vol.* 103, *pp.* 207–223
Printed in Great Britain

Hydrodynamic fragmentation of drops

By P. D. PATEL† AND T. G. THEOFANOUS
Purdue University, West Lafayette, Indiana 47907

(Received 19 June 1979 and in revised form 10 April 1980)

Studies of the morphology of fragmentation of liquid drops in a liquid medium due to shock-induced flows are reported. For such high-density-ratio and high-interfacial-tension systems, the fragmentation is found to be primarily due to the penetration of the drop by unstable waves. An envelope of conditions which characterize drop breakup in these systems has been deduced. Analytical models, which involve the time constants of both the drop-piercing Taylor instability and the wake-forming shear effects, reflect our experimental results well. In addition, it is found that the mercury/water system studied here should simulate the uranium dioxide/sodium pair, which is of interest in safety studies of fast reactors.

1. Introduction

Sometimes the contact of a hot liquid with a cold one can develop into a rapid thermal interaction in which a significant fraction of the thermal energy in the hot liquid is converted into destructive mechanical work. These interactions are called vapour or thermal explosions and have been observed in nature, for example in so-called 'hydroexplosions' that occur on contact between molten volcanic lava and water, and in industry, where molten metals are inadvertently dropped into troughs of water on the shop floor. The destructive work potential of thermal explosions arises from the vapourization and subsequent expansion of the more volatile cold liquid due to heat transfer from the hot liquid. To obtain a coherent explosion, a coupling of the damaging pressure pulse and the extremely fine and rapid fragmentation required to occur behind it, must exist. The fragmentation process would, in all probability, involve hydrodynamic and thermal considerations applied to a three-component system – the hot liquid, the cold liquid and the vapour of the cold liquid. In the simplest case, a process which is purely hydrodynamic and considers just the hot and cold liquids (a liquid/liquid system) can be envisioned.

Drop fragmentation in shock-induced gas flows has been studied quite extensively. Harper, Grube & Chang (1972), in a theoretical analysis, have uncovered a parameter which controls this drop breakup: the Bond number $Bo = \rho_d a_d r_d^2/\sigma$ where ρ_d, a_d, r_d are the density, acceleration and radius of the drop and σ is the interfacial tension. Experiments (Simpkins & Bales 1972; Reinecke & Waldman 1970) have conformed with the theoretical prediction that the breakup, for $Bo \sim 10^5$, is dominated by drop-piercing Taylor instabilities. For lower, but still substantial, Bond numbers, the fragmentation is characterized by a stripping mechanism which is considerably slower

† Now with Shell Development Company, Houston, Texas 77025.

0022–1120/81/4641–3160 $02.00

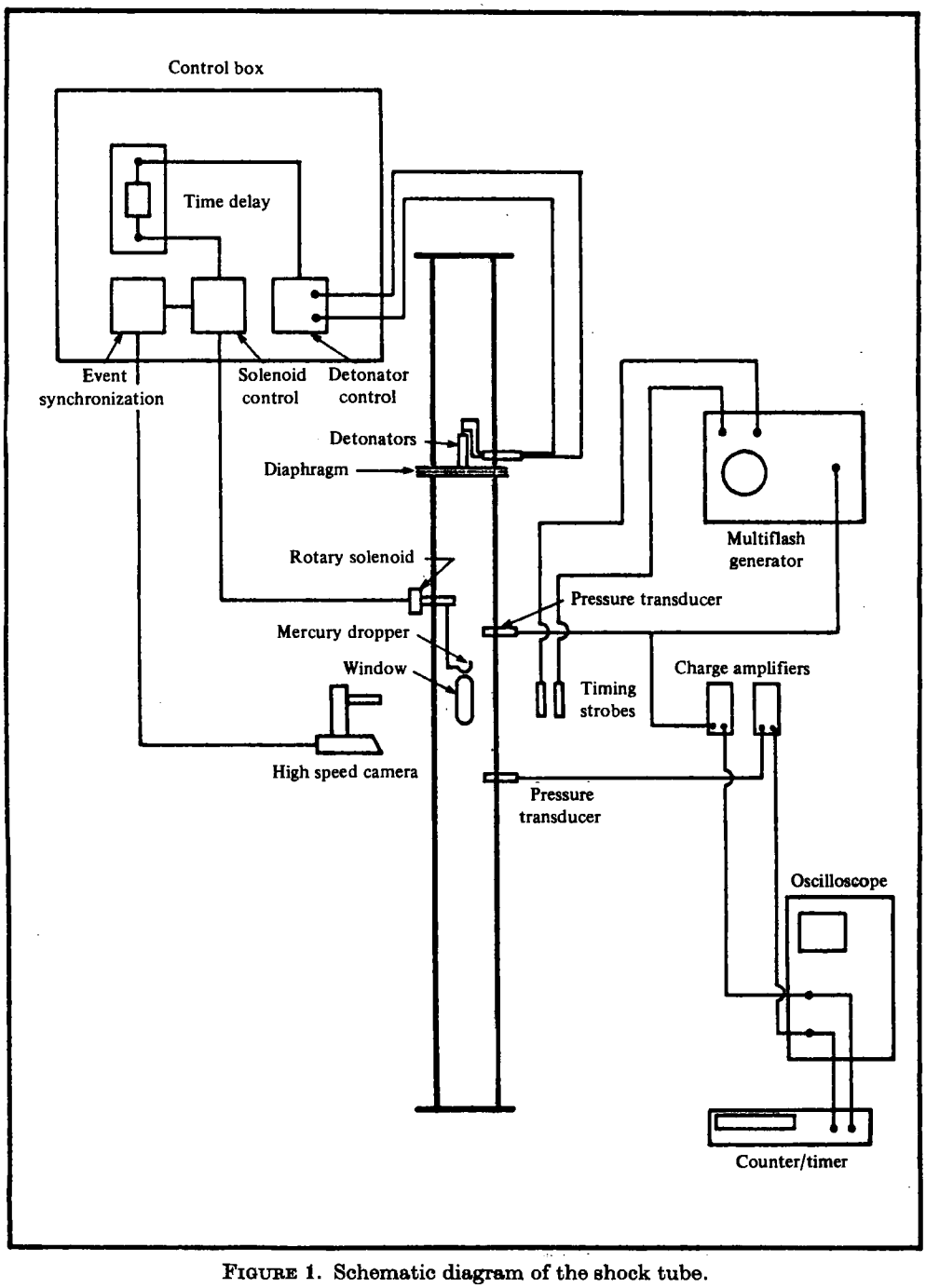

FIGURE 1. Schematic diagram of the shock tube.

in action (Ranger & Nicholls 1969; Reinecke & Waldman 1970) and was first considered by Taylor (1963*a*).

Board, Hall & Hall (1975) have proposed one of the current theories of thermal explosions postulating that the propagation step is due to hydrodynamic fragmentation. In this, as well as several studies that followed this approach fragmentation results from gas/liquid, rather than liquid/liquid, systems were utilized for the simple reason that experiments in the latter system have not been performed as yet. In particular, in relation to the classical air/water data here we are interested in: (*a*) several orders-of-magnitude smaller droplet-to-continuous phase density ratios, (*b*) at least one order higher interfacial tension, (*c*) a continuous phase compressibility similar to that of the drop, and (*d*) highly non-isothermal initial conditions. Our purpose here is to investigate the first three ranges. Such a study of isothermal systems constitutes a necessary step towards isolating any thermal effects.

2. Experimental methods

A hydrodynamic shock tube of 5 cm square cross-section, capable of operation at nitrogen driver pressures in excess of 600 bars, was used. The 300 cm long driven section of the tube was filled with distilled water. Figure 1 is a schematic diagram of the tube and the experimental arrangements. After the camera has been brought up to speed, a signal activates the rotary solenoid which inverts the bucket containing the mercury, gallium or acetylene tetrabromide drop. Following a preset time delay, based on experience, the detonators above the diaphragm are set off automatically leading to diaphragm petalling and subsequent shock-wave formation in the water of the driven section. Except for the earliest experiments, the sensing of the shock wave by the upper piezoelectric pressure transducer (Kislter 601L) was used to trigger a General Radio 1539k strobe driven through a General Radio 1541 Multiflash Generator. This flash serves as a time marker from which the precise instant at which the shock hits the drop can be estimated.

In the first set of experiments, the photographic system used was a Hycam 41-0004 camera, operating at 5000 frames per second, in conjunction with a Pallite VIII lighting unit. Both front-lit and back-lit photography was performed with reversal-acetate and negative-ester based film. In the final set of experiments we were able to use a Beckman and Whitley 375 rotating drum and mirror framing camera at speeds up to 150000 frames per second. The associated Model 359 Flsh Lamp System had a 1100 Joule flash capability for durations between 0·5 and 11 ms. With this system, 500 frames of the event were obtained at extremely short exposure times. All the photography utilized an Elgeet 100 mm f/2·7 lens.

Bond number computations involve the particle velocity behind the shock wave and this is obtained from the pressure history sensed by the transducers. For the driver pressures involved, the shock wave moves at the sonic velocity c in water and the particle velocity u can be obtained from (Cole 1948)

$$\Delta p = \rho u c, \tag{1}$$

where Δp is the pressure differential across the shock and ρ the density of the water behind it. The pressure history in a typical experiment is shown in figure 2. A sharp pressure increase to a constant level is evidenced in all such histories and the duration

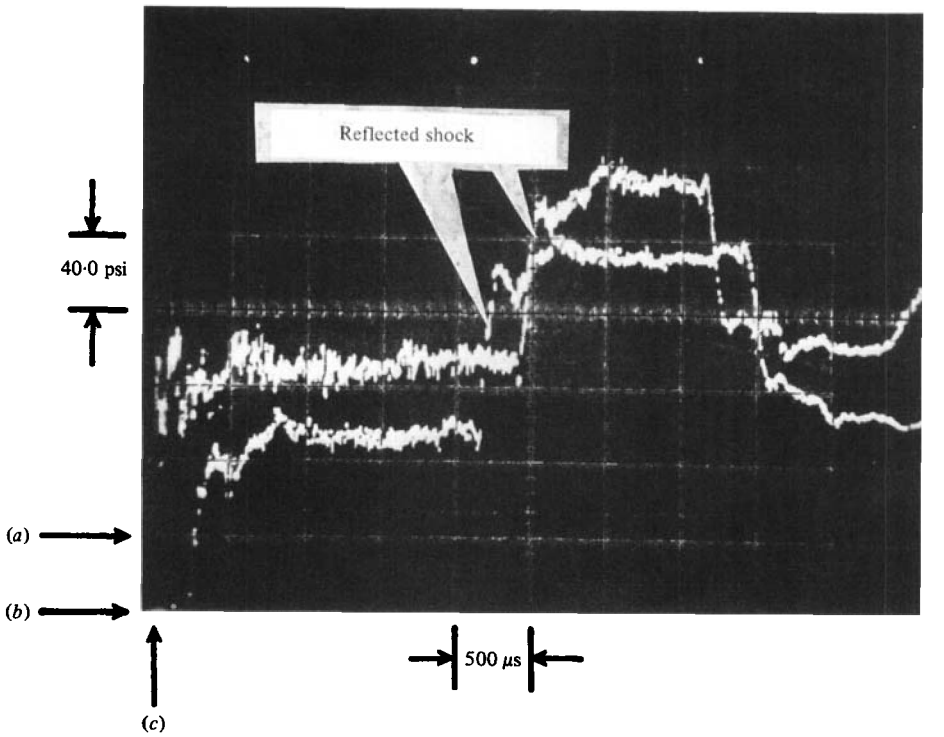

FIGURE 2. Typical pressure transient shape in the shock tube. $Bo = 48$. (a) Upper transducer trace origin. (b) Lower transducer trace origin. (c) Time origin, i.e. instant shock hits upper transducer.

of uniform flow is about 2 ms. The characteristics of figure 2 can be predicted closely by constructing the wave diagram for the shock tube using the Riemann invariant technique (Patel 1978). Considerations described in Glass & Heuckroth (1963) were very useful in analyzing the flow field in the hydrodynamic shock tube.

3. Drag coefficient measurements

Most of the available drag coefficient measurements of distorting water drops in high velocity air flow have been reported by Simpkins & Bales (1972). The consensus is that these drops exhibit a C_D of approximately 2·5 in the Reynolds-number range 10^3–10^5. The acceleration of these drops is found to be constant till breakup. For a liquid/liquid system, however, a considerable decrease of drop acceleration with time may be experienced and the estimation of drag coefficient must consider this. The appendix outlines a method for drag coefficient calculations in such systems. In those experiments amenable to a drag coefficient calculation, we have followed this method and the results are presented in figures 3 and 4. No conclusive estimate of the drag coefficient of fragmenting mercury drops can be made from figure 3. As will be described later, these drops blow up rapidly both transverse to and in the flow direction. Tenuously, it might be concluded that a drag coefficient of 2·5, before substantial breakup sets in, is not unreasonable. Figure 4 shows the results from the acetylene tetrabromide

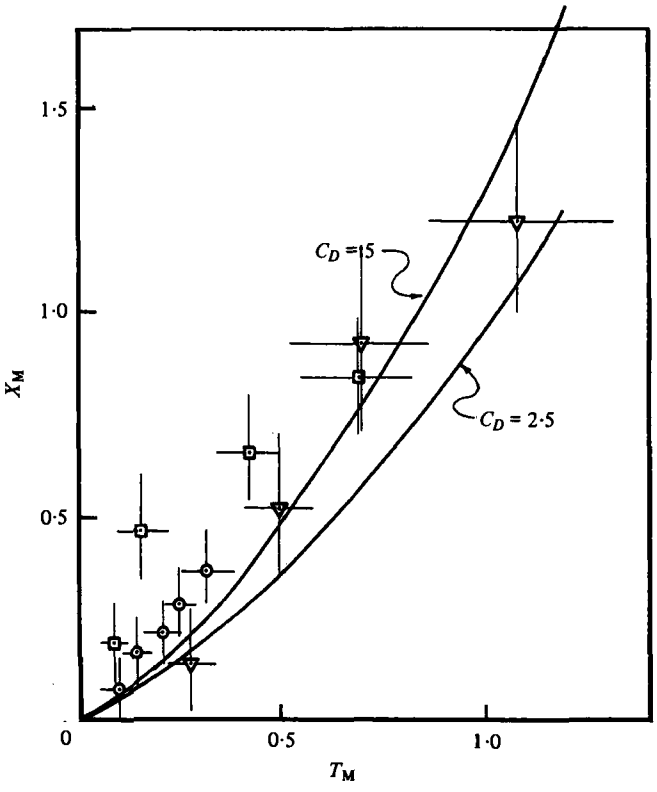

FIGURE 3. Dimensionless displacement (of forward stagnation point) versus time. $X = x/2r_0$, $T = (tu/2r_0)\,\epsilon^{-\frac{1}{2}}$, mercury/water. Bo_0: ⊙, 52 ± 14; ⊡, 1044 ± 194; ▽, 435 ± 90.

drops. These did not evidence the catastrophic breakup of the mercury drops and should allow a more correct estimate of the drag coefficient. A drag coefficient of somewhat less than 2·5 can be deduced from the results of figure 4 over a wide range of the dimensionless displacement and time. Finally, the free-fall observation of a mercury drop in water (where no fragmentation complicates the analysis) exhibited a drag coefficient of 2·1. The Reynolds number in all these experiments varied from 10^3 to 10^5.

4. Experimental results and discussion

Figure 5 shows the response of mercury drops to a shock-induced flow at a Bond number of 52. Figure 6 is a composite which shows the response of mercury, gallium and acetylene tetrabromide drops at higher Bond numbers. It is apparent that the responses are diverse. While all our experiments using mercury and gallium drops exhibited a rapid and uniform blowup in all directions, the acetylene tetrabromide drops evidenced large wakes without substantial increase in size transverse to the flow. In fact, this drop response is very much like that of water drops in an air flow where breakup is usually defined when the wake appears diffuse (Ranger & Nicholls 1969). As the mercury and gallium drops did not experience large wake production, this breakup criterion could not be utilized. Also in the catastrophic mode the 'breakup'

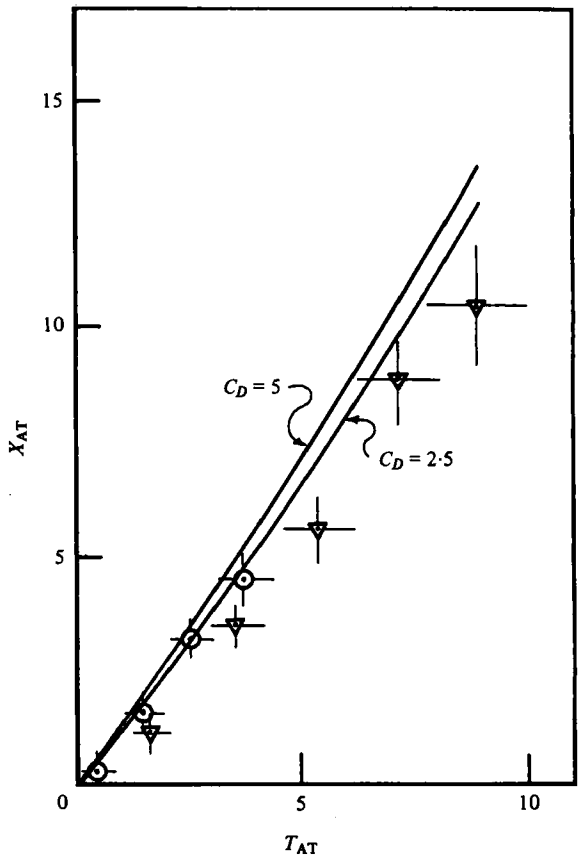

FIGURE 4. Dimensionless displacement (of forward stagnation point) versus time. For acetylene tetrabromide/water. Bo_0: ⊙, 1517 ± 298; ▽, 14310 ± 4200.

time, in gas/liquid systems, has been defined to correspond to total disintegration of the droplet to a *well-dispersed* (diffuse) micromist (Reinecke & Waldman 1970). Again this criterion could not be utilized unambiguously to compare results since the continuous phase flow velocities (and hence rate of dispersion) differ substantially between the two systems. Keeping in mind that for the applications motivating the present study the initial fragment configuration and continuous phase mixing are rather more important we had to resort to a different approach.

We have defined as *breakup*, the time when the drop diameters first show a sudden substantial and continuous increase from their original values. Plots such as figure 7 were used in the break-up-time estimation. Our definition thus is more akin to the initiation of *breakup* rather than the complete disintegration considered by previous workers in this field. An estimation of the time for substantial *fragmentation* is also needed and it can be obtained by associating it with a doubling of the original drop diameter. If fragmentation to the observed level (100–500 μm) is attained throughout the drop conglomerate and if each fragment is contained in a cube of water with side almost twice the fragment diameter, a doubling of the original drop diameter would result. The *breakup* time and the envelope which describes substantial *fragmentation*

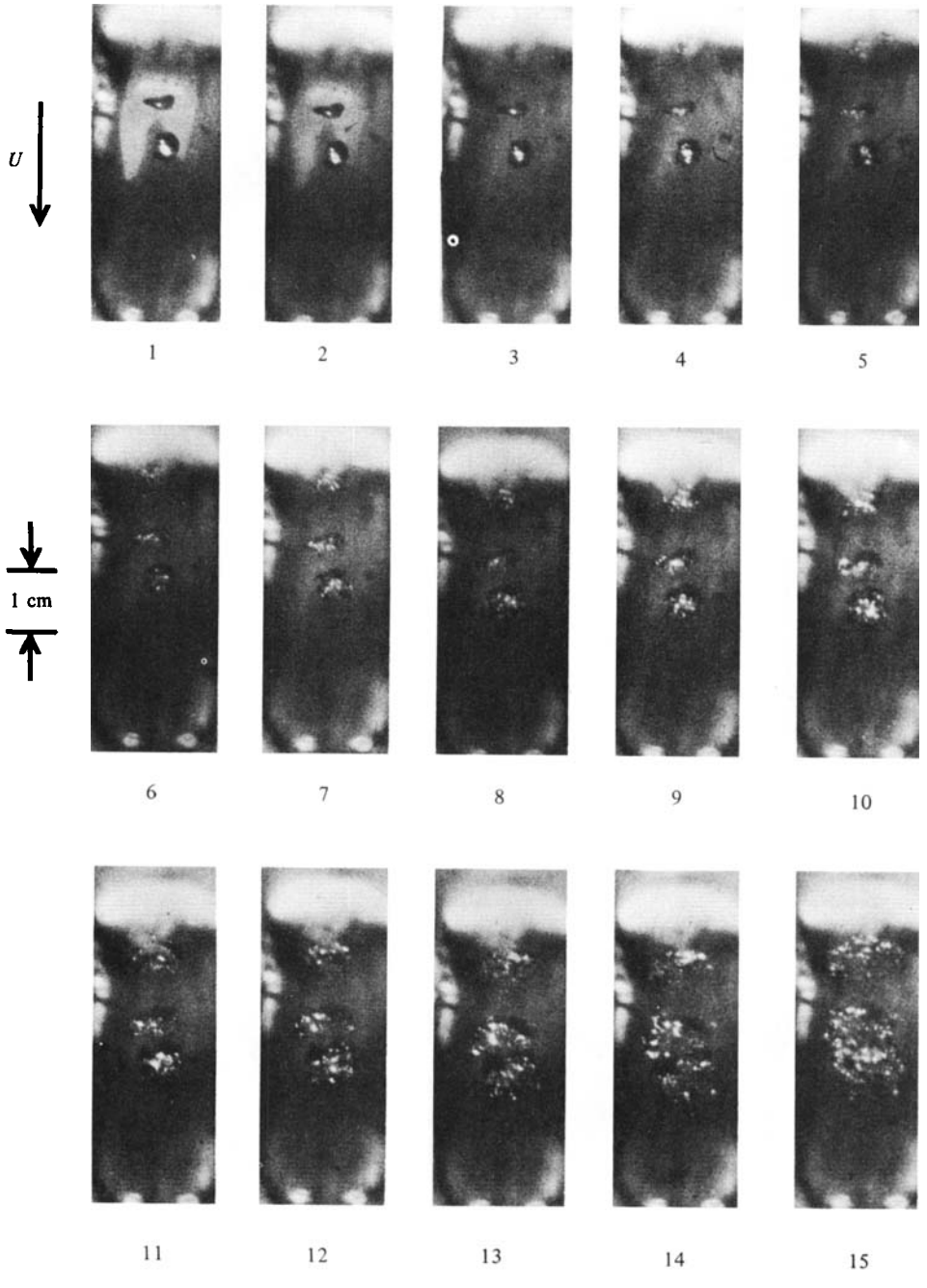

FIGURE 5. Photographic sequence showing the mercury drop response to the shock-induced flow in water. $Bo = 52$. The shock is at the upper pressure transducer sometime during frame 1. Time separation between each frame 1–10 = 220 μs; between each frame 10–15 = 440 μs.

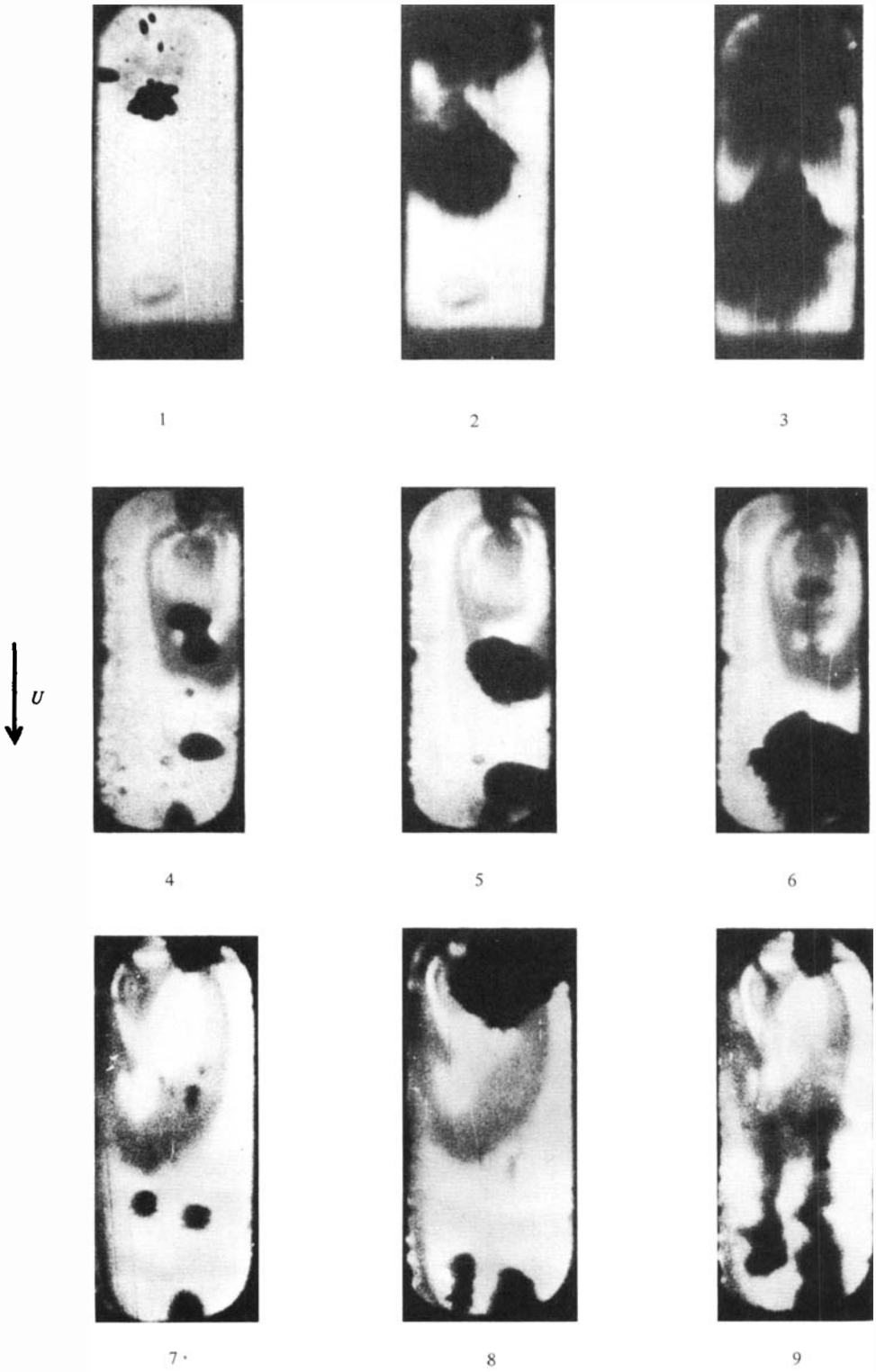

FIGURE 6. For legend see opposite page.

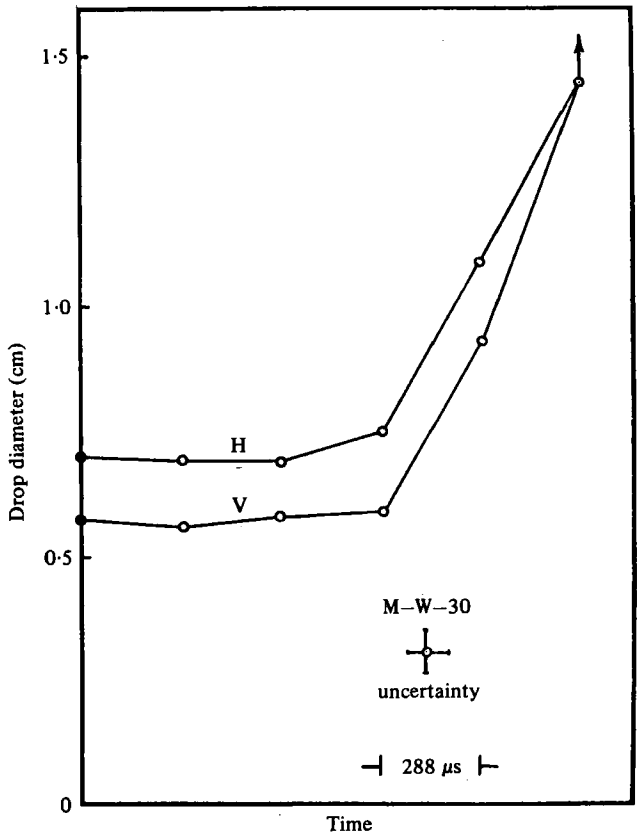

FIGURE 7. M-W-30 diameter history. *H* denotes the horizontal diameter, *V* the vertical diameter.

for the mercury/water experiments is shown in figures 8(*a*, *b*) respectively. The *breakup* time is seen to correspond well with one time constant of the unstable Taylor wave growth given by

$$\tau_b^* = \tau_b \frac{u}{r_d} = 1{\cdot}66\, Bo^{-\frac{1}{2}} \epsilon^{\frac{1}{2}} \tag{2}$$

(where τ_b is the *breakup* time, u is the initial relative velocity and ϵ is the dispersed-to-the-continuous density ratio). Substantial *breakup* seems to correlate well with four Taylor time constants (figure 8*b*). This instability is recognized as the drop-piercing mechanism in the previously reported studies of Reinecke & Waldman (1970),

FIGURE 6. A comparison of the response of mercury, gallium and acetylene tetrabromide drops. 1–3, Mercury/water, shock pressure ratio = 340, largest drop average original diameter = 0·63 cm, Bo_i = 2180: 1, just before shock hits; 2, τ = 720 μs (τ^* = 4·39); 3, τ = 1296 μs (τ^* = 7·90). 4–6, Gallium/water, shock pressure ratio = 420, largest drop average original diameter = 0·82 cm, Bo_i = 4100; 4, just before shock hits; 5, τ = 711 s (τ^* = 4·48); 6, τ = 1422 s (τ^* = 8·96). 7–9, Acetylene tetrabromide/water, shock pressure ratio = 416, left drop average original diameter = 0·19 cm, Bo_i = 13 900: 7, τ = 603 s (τ^* = 9·04); 8, τ = 1005 s(τ^* = 15·09); 9, τ = 5371 s (τ^* = 80·6). Frame 9 includes effects of various reflected waves. $\tau^* = tu/r_d$.

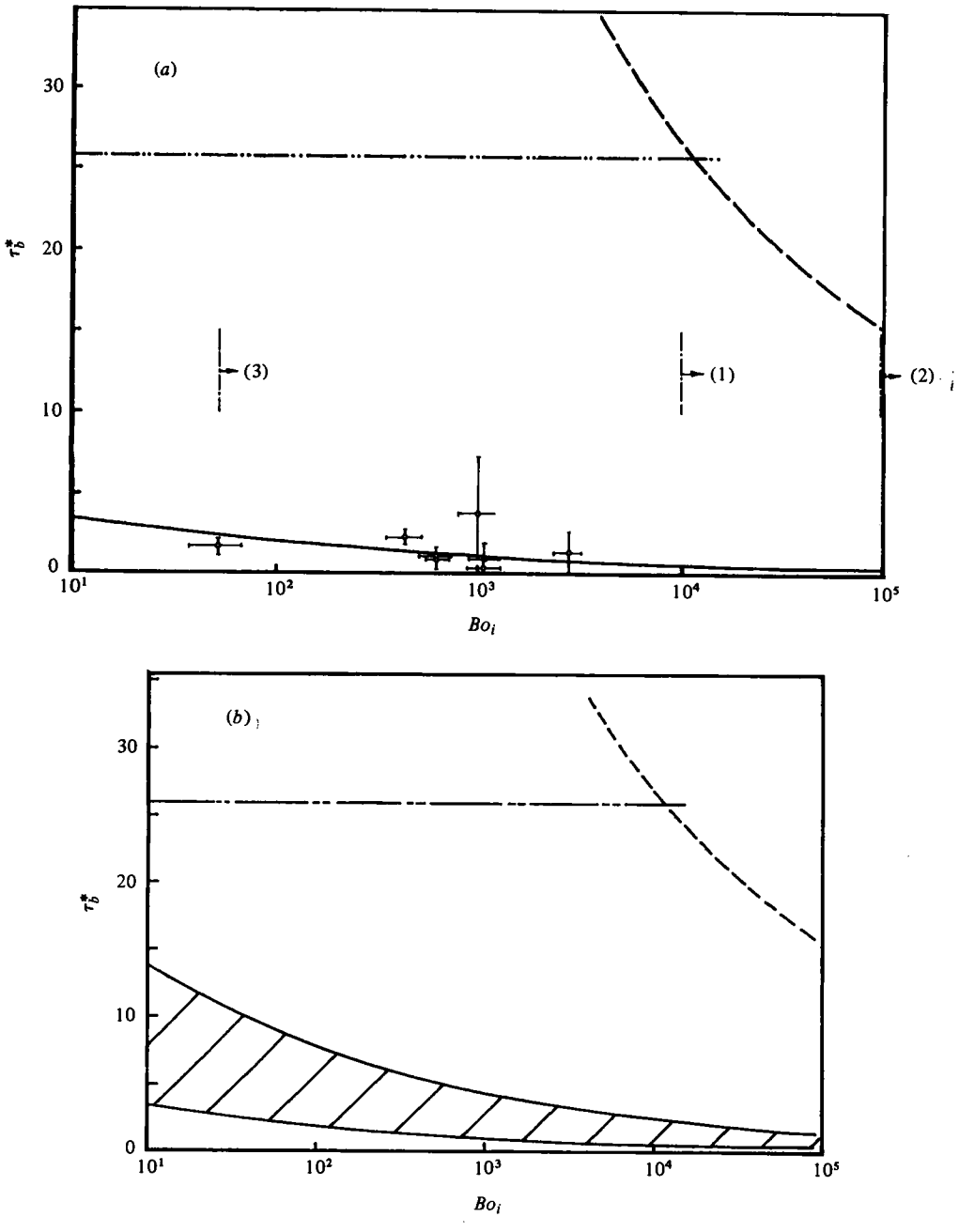

FIGURE 8. (*a*) Dimensionless breakup time versus the initial Bond number for the mercury/water pair. —··—, stripping correlation; – – –, catastrophic breakup correlation; ——, equation (2). (1) Experimental exponential breakup threshold for gas/liquid pairs; (2) theoretical exponential breakup threshold for gas/liquid pairs; (3) instability limit of present work. (*b*) The experimental breakup envelope for the mercury/water pair. —·–·—, stripping correlation; - - - - -, catastrophic breakup correlation, Reinecke & Waldman (1970). The lower and upper bounds of the envelope correspond well to one and four Taylor time constants, respectively, as given by (2).

Simpkins & Bales (1972) and Harper *et al.* (1972) at high Bond numbers. For our experiments, however, the instability correlates the entire range of Bond number and no threshold behaviour between the viscous shearing (or stripping) mode and the instability mode, as observed in gas/liquid systems, is discerned. The correlations obtained in these systems have been extrapolated to the mercury/water pair and are also shown in figure 8. They predict substantially higher breakup times than observed in our experiments.

The conformity of our data with the Taylor time constant given by (2) is an indication that fragmentation may have occurred owing to drop penetration by unstable Taylor waves. Observation of this piercing is difficult and tenuous even in the particular water/air cases where it has been cited as the controlling mechanism. Conclusive evidence and quantification of the particularly important early fragmentation period is not available even for those few air/water cases for which X-ray visualization was employed (Reinecke & Waldman 1970). Such information can only be deduced from time-wise variation in drop mass distributions; we are presently pursuing this goal by means of flash X-ray diagnostics. On the other hand the limitation of the presently employed photographic information must be recognized as such. In this context the apparent discrepancies evidenced in figures 8(*a*, *b*) must be considered with caution.

As a consequence of the high interfacial tension of the mercury and gallium drops, and our experimental technique employed in their formation, free-fall (rpior to shock impact) Weber numbers are of order one. This implies, and the observations confirm, highly convoluted, oscillating, drops. In contrast the free-fall Weber numbers in the air/water experiments were of order 0·1. This implies, and published photos confirm, completely spherical, overstabilized one would say, drops. The importance of the initial perturbation in the initial development and growth of instabilities has been well documented in the past. We would expect it also to play a significant role here in amplifying any other differences between the two different systems.

5. Analysis

We will base our analysis on the view that the primary physical interaction of significance is a result of the 'normal' and 'parallel' components of the external flow field in relation to the drop surface. The normal flow field will predominate near the forward stagnation point and will give rise (during the accelerating phase) to penetrating Taylor waves. The 'parallel' flow field will dominate near the equator and will give rise to a viscous shear layer superposed with travelling with the flow and amplifying, perhaps even entraining, Kelvin–Helmholtz waves. Contributions from both of these two types of physical processes are envisioned for the intermediate positions. We will refer to the two corresponding fragmentation mechanisms as 'piercing' and 'stripping'† respectively and in general both would be expected to participate and interact. For example if the Taylor waves were to be displaced toward the equator more rapidly than the time required for their substantial growth (piercing) the forward drop surface would be continually renewed and stripping would dominate fragmentation. In the other extreme if the growth of Taylor waves is faster than their displacement 'piercing' would dominate. Although each one of these two mechanisms has been acknowledged

† We imploy here the term for all fragmentation resulting from the parallel flow, while classical usage referred only to viscous boundary-layer stripping.

before, the significance of their direct interaction seems to have escaped attention. For example the transition to the catastrophic mode of breakup ('piercing') has been viewed by Harper *et al.* (1972) as the interaction between the growth of Taylor instabilities and drop deformation due to the external (flow-induced) pressure field. We believe that the aerodynamic flattening of the drop would play an indirect role in augmenting the Taylor instabilities by (*a*) increasing the relative proportion of the drop surface subjected to the 'normal' component of the flow field and (*b*) decreasing the distance to which Taylor waves would have to grow to affect complete penetration.

Our purpose here is to give an admittedly crude analysis but one that retains what we believe to represent the essential physical features of the problem. We are aiming primarily at quantifying the relative dominance of the two fragmentation mechanisms rather than exploring the details of each. In this spirit we utilize here the linear Taylor wave growth and a non-deforming drop but note that similar results may be obtained by taking into account nonlinear growth together with aerodynamic flattening. Also in the formulation of the Kelvin–Helmholtz instabilities we assume quasi-stationarity, i.e., the time constant of the instability development is short compared to the time constant for accelerating the drop as a whole, as indeed is the case.

The Taylor instability (see, for instance, Bellman & Pennington 1954) wave amplitude η grows as

$$\eta = \eta_0 \cosh(nt), \tag{3}$$

where n, for fastest growth, is given by

$$n^2 = \tfrac{2}{3}(3\sigma)^{-\frac{1}{2}}[a(\rho_2-\rho_1)]^{\frac{3}{2}}(\rho_2+\rho_1)^{-1} \tag{4}$$

and a is the imposed acceleration and ρ_1 and ρ_2 the densities of the lighter and heavier fluids respectively. The time constant τ_T, characterizing the instability growth is

$$\tau_T = 1/n. \tag{5}$$

The Kelvin–Helmholtz instability (see Chandrasekhar 1961, pp. 483 ff), which considers two uniform, incompressible, inviscid fluids of densities ρ_1 and ρ_2 streaming with constant velocities U_1 and U_2 in the direction x of their interface, is characterized by a wave amplitude, η, growth from initial perturbation η_0 given by

$$\eta = \eta_0 \cos K_r\left(x + \frac{n_r}{K_r}t\right) e^{n_i t} \tag{6}$$

where

$$\frac{n_r}{K_r} = -C = \frac{\rho_1}{\rho_1+\rho_2}U_1 + \frac{\rho_2}{\rho_1+\rho_2}U_2 \tag{7}$$

represents the propagation velocity of the growing wave and

$$n_i = [BK_r^2 - AK_r^3]^{\frac{1}{2}}, \tag{8}$$

where

$$A = \frac{\sigma}{\rho_1+\rho_2}, \quad B = \frac{\rho_1\rho_2}{(\rho_1+\rho_2)^2}(U_1-U_2)^2 \tag{9), (10}$$

represents the rate of growth of wave amplitude. For the fastest such growth,

$$n_{i\,\max} = \left\{\frac{4B^3}{27A^2}\right\}^{\frac{1}{2}} \tag{11}$$

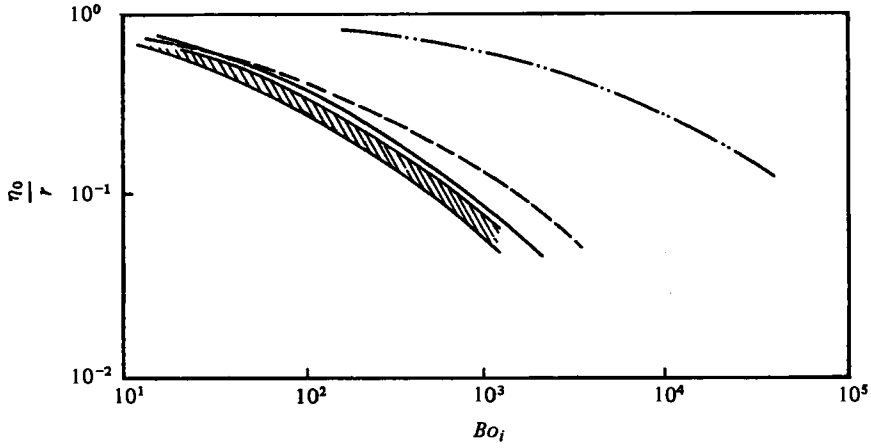

FIGURE 9. Results from the physical model. —··—, acetylene tetrabromide/water; – – –, gallium/water; ——, mercury/water; ▨, uranium dioxide/sodium.

and the time constant τ_H is

$$\tau_H = \frac{1}{n_{i\,\max}}. \tag{12}$$

A physical model

This model considers penetration by Taylor instability and wake formation by Kelvin–Helmholtz waves riding on the boundary layer in the drop and suffering subsequent separation from its surface. The boundary-layer analysis follows that of Taylor (1963*a*) and Ranger & Nicholls (1969) but the liquid/liquid systems considered here require an iterative solution of the equations. The time for the shear wave to travel from the windward and stagnation point on the drop to its equator was computed and the initial perturbation η_0 which allows the Taylor wave to penetrate from that stagnation point to the drop centre *in the same time* was deduced. The scale of values of η_0 can best be regarded as a measure of the relative dominance of the two instabilities: a diminution of η_0 being indicative of an increase in the dominance of the Taylor instability.

The results of this model are presented in figure 9. For realistic initial perturbations (say $\eta_0/r < 0{\cdot}1$), a Taylor instability dominance is indicated for mercury/water at $Bo \sim 500$ while a similar dominance for the acetylene tetrabromide/water pair would only assert itself for $Bo > 50\,000$. This result is in consonance with our experimental findings. Further, figure 9 shows that the mercury/water pair is a good simulant of the drop response morphology in the uranium dioxide/sodium system which is of current interest in fast reactor safety studies. It must be emphasized that the trends of figure 9 should only be used to make conclusions regarding the *relative* responses of the different systems. Any absolute determinations made would be injudicious as the underlying phenomena have been considered in some simplicity.

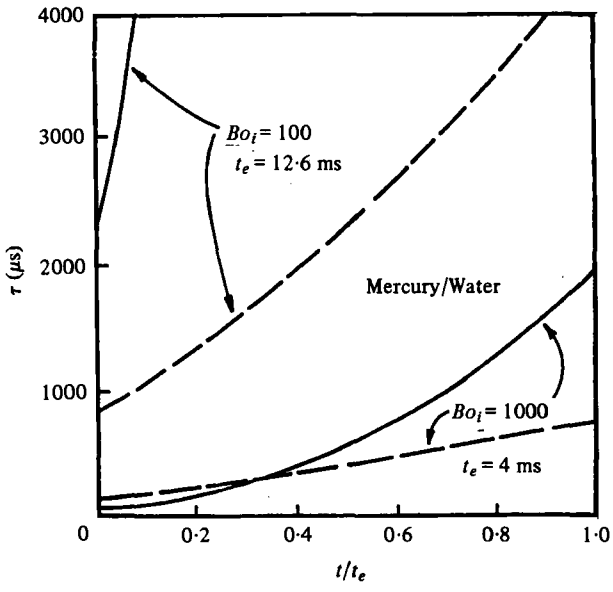

FIGURE 10. Time constant history for mercury/water. ——, $50\tau_H$; – – –, τ_T. Drop radius = 0·2 cm.

A time constant history model

This model considers the ratio of the instability time constants, τ_H and τ_T, as determining the drop response. The wake formation is assumed to result from the undercutting by the flow of large-amplitude Kelvin–Helmholtz waves and the deposition of the cropped material behind the main drop mass. It has already been established that the mercury drop breakup time is well correlated by one time constant of the Taylor instability process. A similar relation between the Kelvin–Helmholtz time constant and the inception of the wake can be approximated from an acetylene tetrabromide run. The wake inception follows after approximately $50\tau_H$.

The diminution of Bond number with time, which results from the decrease in drop acceleration, can be expressed (under the assumption of constant drag coefficient) as

$$\frac{Bo}{Bo_i} = \left(\frac{u-v}{u-v_i}\right)^2, \tag{13}$$

where v_i is the initial drop velocity, v the drop velocity at time t and u the free-stream velocity. Using the drop equilibration time t_e, which can be chosen to correspond to $v = 0{\cdot}7u$, we can obtain, on substitution of the property values, and (A 4) for the mercury/water pair,

$$\{Bo_i/Bo\}_{\mathrm{M-W}} = (2t/t_e + 1)^2 \tag{14}$$

and for the acetylene tetrabromide/water pair,

$$\{Bo_i/Bo\}_{\mathrm{AT-W}} = (\tfrac{2}{3}t/t_e + 1)^2. \tag{15}$$

The ratio of the time constants is, for $\rho_2 \gg \rho_1$,

$$\tau_T/\tau_H = 0{\cdot}65\, We^{\frac{1}{4}} \tag{16}$$

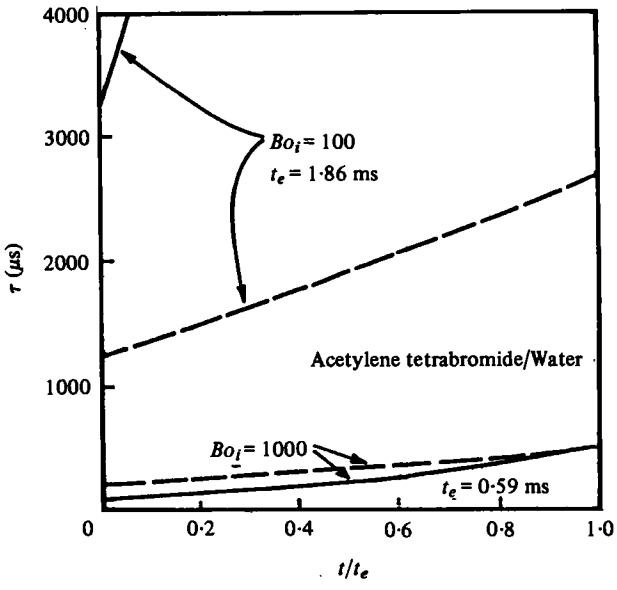

FIGURE 11. Time constant history for acetylene tetrabromide/water. ——, $50\tau_H$; – – –, τ_T. Drop radius = 0·1 cm.

where $We = \rho_1 u^2 r_0 \sigma^{-1}$ is the well-known Weber number. On substitution of property values into the expression for τ_T and τ_H given by (5) and (12) and using the Bond number variation of (14) and (15), we get

$$(\tau_T)_{\text{M-W}} = 0{\cdot}3\left\{\frac{Bo_i}{(2t/t_e+1)^2}\right\}^{-\frac{3}{4}} r_0^{\frac{3}{2}} \quad \text{(s)}, \tag{17}$$

$$(\tau_T)_{\text{AT-W}} = 1{\cdot}25\left\{\frac{Bo_i}{(\frac{2}{3}t/t_e+1)^2}\right\}^{-\frac{3}{4}} r_0^{\frac{3}{2}} \quad \text{(s)}, \tag{18}$$

$$50(\tau_H)_{\text{M-W}} = 25\left\{\frac{Bo_i}{(2t/t_e+1)^2}\right\}^{-\frac{3}{4}} r_0^{\frac{3}{2}} \quad \text{(s)}, \tag{19}$$

$$50(\tau_H)_{\text{AT-W}} = 105\left\{\frac{Bo_i}{(\frac{2}{3}t/t_e+1)^2}\right\}^{-\frac{3}{4}} r_0^{\frac{3}{2}} \quad \text{(s)}, \tag{20}$$

where r_0 is in cm. Figures 10 and 11 show the time constant histories for two Bond numbers 100 and 1000. By choosing a value of t/t_e it can be ascertained whether the drop-piercing by unstable waves, wake formation or both should manifest themselves at the particular Bond numbers. These predictions conform with our experimental observations very well except for the high Bond number acetylene tetrabromide/water case where the proximity of the time constants and the real time renders any conclusion hazy.

6. Conclusions

The conclusions drawn are:

(*a*) For the mercury/water system and freely falling large drops there does not appear to be a Bond number threshold which controls drop response as for the water/air pair.

(*b*) One time constant for the growth of unstable Taylor waves correlate the breakup time in the mercury/water system quite well through the entire Bond-number range investigated, i.e. 52–2810. An envelope which includes one to four Taylor time constants is representative of substantial fragmentation in the mercury/water system.

(*c*) A drag coefficient of 2·5, under shock induced flow conditions in the Reynolds-number range 10^3–15^5, is not unreasonable for liquid/liquid systems.

(*d*) The results of theoretical schemes which pit the drop piercing Taylor instability against the wake-forming shear instability reflect experimental behaviour well.

(*e*) The fragmentation of mercury drops in water probably simulates that of UO_2 drops in sodium quite closely.

(*f*) Substantial fragmentation of UO_2 drops in sodium may not require as strong a shock wave as had been expected on the basis of previous work.

This work was performed for the U.S. Nuclear Regulatory Commission under contract no. NRC-03-76-181. The arrangements provided by Dr H. K. Fauske for borrowing the Beckman–Whitley camera from Argonne National Laboratory and the assistance of Dr D. Armstrong in learning its use are gratefully acknowledged. F. Koontz helped with the automatic synchronization system.

Appendix. The drag coefficient calculations

For a spherical drop of radius r_0 and density ρ_d moving at velocity V in a flow of constant velocity u and density ρ_c, the balance of forces is (buoyancy and virtual mass effects taken together are negligible)

$$(\tfrac{4}{3}\pi r^3\rho_d)\,a = \tfrac{1}{2}\rho_c(u-V)^2 C_D(\pi r_0^2) \tag{A 1}$$

or, the acceleration a is given by

$$a = \frac{dV}{dt} = \frac{3}{8}\frac{\rho_c}{\rho_d}\frac{C_D}{r_0}(u-V)^2 = \beta(u-V)^2, \tag{A 2}$$

where

$$\beta = \frac{3}{8}\frac{\rho_c}{\rho_d}\frac{C_D}{r_0} \equiv \frac{3}{8}\frac{1}{\epsilon}\frac{C_D}{r_0}. \tag{A 3}$$

For initial velocity of the drop V_0 velocity V at time t, is obtained as:

$$V = \frac{dx}{dt} = u - \frac{(u-V_0)}{\beta(u-V_0)\,t+1}, \tag{A 4}$$

where x is the displacement of the drop. Integrating (A 4) we obtain for the displacement x at time t,

$$x = ut - \frac{1}{\beta}\ln\{(u-V_0)\,\beta+1\}, \tag{A 5}$$

or in dimensionless form ($X = x/2r_0$ and $T = (ut/2r_0)\,\epsilon^{-\frac{1}{2}}$),

$$X = T\epsilon^{\frac{1}{2}} - \frac{4}{3}\frac{\epsilon}{C_D}\ln\left\{\left(\frac{u-V_0}{u}\right)\frac{3}{4}\frac{C_D}{\epsilon^{\frac{1}{2}}}T+1\right\}. \tag{A 6}$$

This is intended only as an order-of-magnitude estimate for fragmenting and deforming drops (i.e., mass and drag coefficients may vary with time.)

REFERENCES

BELLMAN, R. & PENNINGTON, R. H. 1954 *Quart. Appl. Math.* **12**, 151.

BOARD, S. J., HALL, R. W. & HALL, R. S. 1975 *Nature* **254**, 319.

CHANDRASEKHAR, S. 1961 *Hydrodynamic and Hydromagnetic Stability*. Clarendon.

COLE, R. H. 1948 *Underwater Explosions*. Princeton.

GLASS, I. I. & HEUCKROTH, L. E. 1963 *Phys. Fluids* **6**, 543.

HARPER, E. Y., GRUBE, G. W. & CHANG, I. 1972 *J. Fluid Mech.* **52**, 565.

PATEL, P. D. 1978 Hydrodynamic fragmentation of drops. Ph.D. thesis.

RANGER, A. A. & NICHOLLS, J. A. 1969 *A.I.A.A. J.* **7**, 2.

REINECKE, W. R. & WALDMAN, G. 1970 *Proc. 3rd Int. Conf. Rain Erosion and Associated Phenomena*, p. 629.

SIMPKINS, P. G. & BALES, E. L. 1972 *J. Fluid Mech.* **55**, 629.

TAYLOR, G. I. 1963*a* The shape and acceleration of a drop in a high-speed air stream. *Scientific Papers of G. I. Taylor* (ed. G. K. Batchelor), vol. III. Cambridge University Press.

TAYLOR, G. I. 1963*b* The instability of liquid surfaces when accelerated in a direction perpendicular to their planes. I. *Scientific Papers of G. I. Taylor* (ed. G. K. Batchelor), vols. I, III. Cambridge University Press.